River Bathymetry Retrieval From Landsat-9 Images Based on Neural Networks and Comparison to SuperDove and Sentinel-2

Milad Niroumand-Jadidi, *Member, IEEE*, Carl J. Legleiter, and Francesca Bovolo, *Senior Member, IEEE*

***Abstract*—The Landsat mission has kept an eye on our planet, including water bodies, for 50 years. With the launch of Landsat-9 and its onboard Operational Land Imager 2 (OLI-2) in September 2021, more subtle variations in brightness (14-bit dynamic range) can be captured than previous sensors in the Landsat series (e.g., 12-bit Landsat-8). The enhanced radiometric resolution of OLI-2 appeals to the aquatic remote sensing community because the instrument might be capable of resolving smaller differences in water-leaving radiance. This study evaluates the potential to map river bathymetry from Landsat-9 imagery. We employ a neural network (NN)-based regression model for bathymetry retrieval and compare the results with optimal band ratio analysis (OBRA). The effect of Landsat-9 pan-sharpening on depth retrieval is also examined. In addition, we perform an intersensor comparison with Sentinel-2 and newly available 8-band SuperDoves from the PlanetScope constellation. Depth retrieval results from the Colorado and Potomac Rivers imply that Landsat-9 provided more accurate bathymetry across a range of depths up to 20 m, particularly when pan-sharpened. Downsampling the SuperDove data improved bathymetry retrieval due to enhanced signal-to-noise ratio, most notably in deep waters (maximum detectable depth increased from ∼15 to ∼20 m). Similarly, the enhanced spectral resolution of 8-band SuperDoves improved depth retrieval relative to 4-band Doves. The NN-based model outperformed OBRA by incorporating more spectral information.**

***Index Terms*—Bathymetry, CubeSats, landsat-9, machine learning, neural networks (NNs), pan-sharpening, planetscope, rivers, sentinel-2, superdove.**

I. Introduction

THE Landsat satellite mission is well-known as the longest continuous means of monitoring Earth resources from space, dating back to 1972. The sensors onboard Landsat satellites have evolved significantly over the past five decades [1]. Since the launch of Landsat-8 in 2013, retrieval of biophysical parameters, such as water quality and bathymetry in inland and nearshore coastal waters has entered a new era enabled by the enhanced radiometric resolution relative to previous sensors (i.e., 12-bit versus 6–8-bits) [2], [3]. Radiometric resolution is particularly important in aquatic applications given the low signal-to-noise ratio (SNR) over water bodies due to strong absorption of downwelling irradiance by pure water [4], [5]. The new Landsat-9 carrying the Operational Land Imager 2 (OLI-2) goes a step beyond the OLI aboard Landsat-8 by providing data with a 14-bit dynamic range. The improved radiometric resolution of OLI-2 could open up new opportunities for monitoring inland and coastal waters by providing higher sensitivity to water-leaving radiance. Similar to OLI, OLI-2 captures visible, near, and shortwave- infrared bands at 30-m spatial resolution, along with a 15-m panchromatic band. This study presents the first evaluation of the potential of the new Landsat-9 mission for bathymetry retrieval in fluvial systems. The spatially and temporally distributed bathymetric information provided by space-borne remote sensing plays an indispensable role in hydro-morphological studies, as well as stream habitat assessment and ecological modeling [6], [7].

We perform an intersensor comparison to quantify the depth retrieval performance of Landsat-9 relative to Sentinel-2 and CubeSat data from the PlanetScope constellation. Eight-band SuperDove data have been made available only recently, and thus, this study also presents the first analysis of the utility of this type of PlanetScope data for river bathymetry retrieval. SuperDove CubeSats provide four additional bands compared to standard Doves. Both Dove and SuperDove CubeSats provide daily and sometimes subdaily imagery at ∼3-m spatial resolution. The unprecedented high spatiotemporal resolution of PlanetScope CubeSats can facilitate near real-time monitoring of inland water bodies, including small rivers [8]–[10]. The enhanced spectral resolution offered by SuperDoves makes these new CubeSats more conducive to aquatic applications. Although Doves and SuperDoves capture spectral information with 12-bit radiometric resolution, concerns have been raised regarding the radiometric quality of CubeSat data because the sensors are small and inexpensive [9], [11]. The multispectral imager (MSI) onboard Sentinel-2A/B, also considered in this study, is another satellite-based instrument that has been utilized for aquatic remote sensing because it provides suitable spatial (10−20-m), radiometric (12-bit), spectral (13 bands), and temporal (2–3 days) resolutions [12]. Thus, three sensors covering a wide range of spatial and spectral resolutions are evaluated in the intersensor comparison.

Manuscript received 13 April 2022; revised 21 May 2022; accepted 26 June 2022. Date of publication 29 June 2022; date of current version 11 July 2022. *(Corresponding author: Milad Niroumand-Jadidi.)*

Milad Niroumand-Jadidi and Francesca Bovolo are with the Digital Society Center, Fondazione Bruno Kessler, 38123 Trento, Italy (e-mail: mniroumand@fbk.eu; bovolo@fbk.eu).

Carl J. Legleiter is with the Observing Systems Division, U.S. Geological Survey, Golden, CO 80403 USA (e-mail: cjl@usgs.gov).

Digital Object Identifier 10.1109/JSTARS.2022.3187179

Spectrally based bathymetry retrieval methods fall into the following two main categories: empirical and physics-based [13], [14]. Empirical approaches rely on training a regression model between image-derived spectral features (e.g., band ratios) and associated *in situ* bathymetry data [15], [16]. Optimal band ratio analysis (OBRA) is a widely used empirical model that seeks an optimal pair of bands, among all possible band combinations, to establish a model for depth retrieval [17]. OBRA is utilized in several studies to map river bathymetry, particularly using high spatial resolution imagery from either airborne sensors [18] or spaceborne instruments, such as WorldView [16]. Empirical models have been used to derive nearshore bathymetry from Sentinel-2 imagery [19]–[21]. Band ratio models have also been applied to Landsat-8 imagery to derive the bathymetry of lakes in northern Alaska [22]. Similarly, polynomial regression models have been applied to PlanetScope 4-band imagery for bathymetry estimation in coastal waters [11], [23]. On the other hand, physics-based approaches invert a radiative transfer model to derive bathymetric information [24]. Radiative transfer simulations are the basis for inversion models that account for absorption and backscattering properties of pure water, in-water constituents, and the substrate [25]–[27]. The observed (image) spectra are compared with simulated spectra generated based on a range of parameters, including water depth, to find the optimal match [28], [29]. To achieve reliable retrievals, physics-based models require precise atmospheric correction of imagery data and need to be parameterized with site-specific inherent optical properties [9]. Empirical and physics-based models have their pros and cons, but the former approach remains a common choice in bathymetric studies, particularly in riverine environments [6], [14], [30]. This study also considered an alternative regression-based depth retrieval model based on machine learning. We leverage neural network (NN)-based models to retrieve bathymetry and compare the results with standard OBRA. NNs are powerful tools for learning complex, nonlinear relations between input features (spectral data) and the target parameter (water depth) [31].

This study pursues the following objectives:

1) examine river bathymetry retrieval from newly available Landsat-9 imagery;
2) perform an intersensor comparison of the depth retrieval capabilities of the new Landsat-9 and SuperDove CubeSats, as well as Sentinel-2;
3) investigate the impact on river bathymetry retrieval of enhancing the spatial resolution of Landsat-9 by pansharpening;
4) isolate the effect of spatial resolution on depth retrieval by resampling imagery from different sensors to a common (15-m) resolution, which also provides insight regarding the impact of enhancing the SNR of CubeSat imagery by downsampling the data;
5) apply a machine learning-based model for depth retrieval from various sensors and compare the results with OBRA.

Section II introduces the studied rivers and associated *in situ* and imagery datasets. The methods, including the NN and OBRA, are described in Section III. The results and discussion are provided in Section IV. Finally, Section V concludes this article.

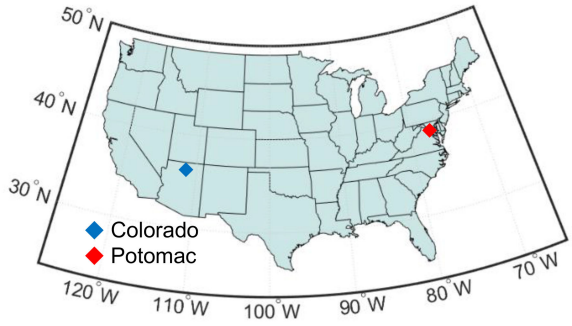

Fig. 1. Location of the studied river reaches on a map of the United States.

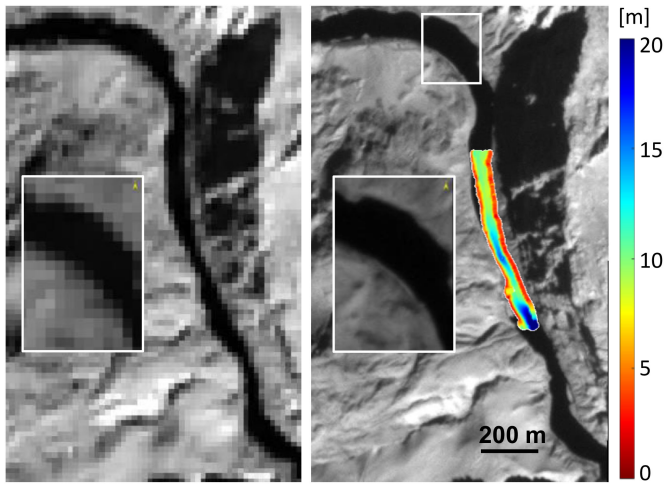

Fig. 2. (a) Landsat-9 (30 m pixels, 865 nm band) and (b) SuperDove (3 m pixels, 866 nm band) imagery of the study area on the Colorado River. The location of the zoomed-in subsets, which are included to show differences in spatial resolution, and the *in situ* depths are shown on the SuperDove image.

II. Case Studies and Datasets

This study used data from two clear-flowing rivers that span a wide range of depths to examine the bathymetry retrieval from Landsat-9 imagery compared to Sentinel-2 and SuperDove. The selected river reaches are located on the Colorado and Potomac Rivers in the United States (see Fig. 1). The selected rivers are relatively wide (∼100 m), and thus, allow for analyzes at different spatial resolutions. The Colorado reach exhibits depths up to ∼20 m, whereas four different reaches with field-measured depths along the Potomac River are up to ∼ 5 m deep. The broad range of water depths provided by the two case studies allows for a thorough cross-sensor assessment of bathymetry retrieval. In addition, these two rivers had very low turbidity, as required for spectrally based depth retrieval [17]. The river reaches and *in situ* data are shown in Figs. 2 and 3. For each studied river, Landsat-9 with the original spatial resolution (30-m) and SuperDove (3-m) images are illustrated to enable visualization of the differences

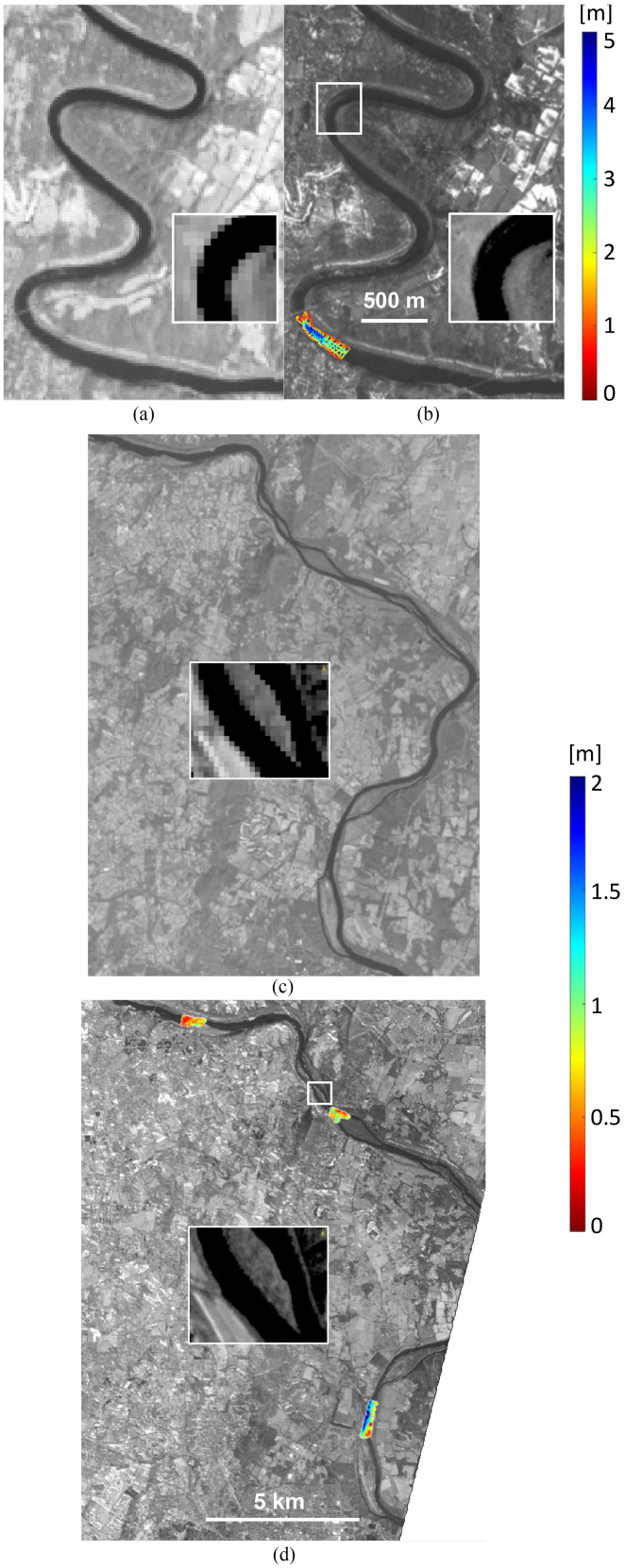

Fig. 3. (a), (c) Landsat-9 (30 m resolution, 865 nm band) and (b), (d) SuperDove (3 m resolution, 866 nm band) imagery of the study area on the Potomac River. The location of the zoomed-in subsets, which are included to show differences in spatial resolution, and the *in situ* depths are shown on the SuperDove image.

TABLE I
CHARACTERISTICS OF THE CASE STUDIES AND A SUMMARY OF THE IMAGERY AND *IN SITU* DATA

	Colorado	Potomac
Characteristics	Clear-flowing, confined river below Glen Canyon; depths up to 20 m surveyed by sonar	Bedrock-controlled channel; depths up to 5 m in multiple study reaches surveyed with an ADCP
Imagery data	Landsat-9, 11 Feb 2022 Sentinel-2, 11 Feb 2022 SuperDove, 11 Feb 2022	Landsat-9, 1 Feb 2022 Sentinel-2, 8 Jan 2022 SuperDove, 1 Feb 2022
Number of field samples (Original and 15-m resolution)	Landsat-9, 147 – 480 Sentinel-2, 989 – 484 SuperDove, 9393 – 481	Landsat-9, 786 – 2162 Sentinel-2, 3563 – 2145 SuperDove, 12106 – 2136

The numbers of field samples are provided for the original and pan-sharpened/resampled resolutions, respectively.

in spatial resolution. One of the Potomac reaches is presented separately for better visualization of the images and *in situ* depths (see Fig. 3).

The *in situ* data from the Colorado River were obtained by performing multibeam sonar surveys on September 23, 2019 [32]. The bathymetric survey at the Potomac River was conducted with a boat-mounted acoustic Doppler current profiler (ADCP) on October 21–24, 2019 [33]. The *in situ* data used in this study and the full description of measurement procedures are available through the USGS ScienceBase Catalog [32], [33]. The selected reaches are regulated by dams, and thus, the discharge is relatively stable over time. In addition, the presence of dams reduces, if not eliminates, sediment transport, and thus, channel changes between the time of field data collection and image acquisition were assumed to be minimal. To account for any possible stage differences between image and *in situ* acquisition dates, we used gage data available from USGS stations in the study sites. There was no change in stage for the Colorado River. Furthermore, all the images of the Colorado (Landsat-9, Sentinel-2, and SuperDove) were acquired on the same day and within an hour of one another, ensuring similar flow conditions for the intersensor comparison. A slight change in stage was identified for the Potomac River. We applied a +0.24-m shift to the *in situ* depths to adjust them to the stage on the Landsat-9 and SuperDove acquisition date. There was no Sentinel-2 overpass on the same day as the other images and slightly a greater adjustment of the *in situ* data was needed for the Sentinel-2 acquisition date (+ 0.54 m). Because the *in situ* data were acquired at a centimeter-scale spatial resolution, the depth measurements inside a given pixel were averaged to match the spectral data at the pixel level for each sensor and spatial resolution. The high density of the field measurements ensured that this approach provided representative pixel-scale mean depths across a range of resolutions from 3 to 30 m. The general characteristics of the river reaches, imagery data, and the number of *in situ* matchups at different spatial resolutions are provided in Table I.

We use top-of-atmosphere reflectance products from Landsat-9, Sentinel-2, and SuperDove satellites. Although bottom-of-atmosphere (BOA) products are also available, they did not

benefit our analyzes and, in some cases, led to degradation of the results due to poor atmospheric correction.

Thus, for brevity, we excluded the BOA data analyzes and results. Previous studies also demonstrated that atmospheric correction is not essential for bathymetry retrieval when applying a regression-based model to a single scene [6]. OLI-2 onboard Landsat-9 provides eight bands within the visible to shortwave infrared (SWIR) portion of the spectrum. However, one of the Landsat-9 bands, centered around 1370 nm, is for detecting clouds, particularly thin cirrus clouds, and was discarded in our analyzes. These multispectral bands are acquired at 30-m resolution, whereas the panchromatic band is acquired with a 15-m resolution. Sentinel-2 (MSI) provides 13 spectral bands in a similar spectral range to OLI-2. Similar to Landsat-9, the band for detecting clouds (∼1370 nm) was discarded. Although the water-leaving reflectance is mainly considered negligible over SWIR bands, they may contain information about sunglint [34], [35]. Thus, we retained the SWIR bands because they might make the NN model more robust to glint effects. SuperDoves capture eight spectral bands spanning the visible and near-infrared (NIR) spectrum. SuperDoves provide four additional bands beyond those included on standard Doves. The additional bands include coastal blue (443 nm), an extra green band (531 nm), a yellow band (610 nm), and a red edge band (705 nm). Although SuperDoves do not capture SWIR bands, this has minimal impact on bathymetric applications, as water-leaving radiance tends to zero at the SWIR portion of the spectrum. The NIR band of SuperDoves can be used instead of an SWIR band for sun glint mitigation [36]. To examine the effect of the additional bands, we perform depth retrieval by removing them from the SuperDove data. The results derived from 4-band SuperDove data are then compared with those of 8-band imagery. The band designation and relative spectral response of the sensors are illustrated in Fig. 4.

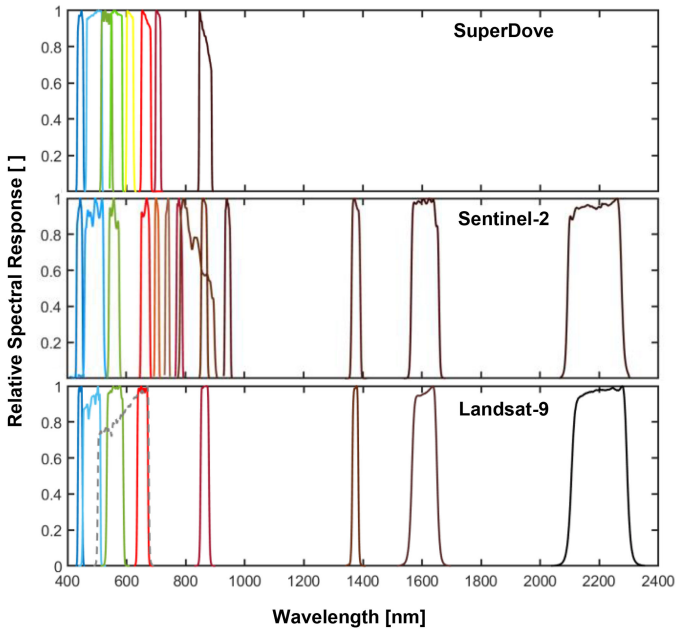

Fig. 4. Relative spectral response of sensors onboard Landsat-9, Sentinel-2, and SuperDove [37]. The gray dashed line shows Landsat-9's panchromatic band.

III. Methods

Regression-based models are widely employed for retrieving river bathymetry from optical imagery. Most studies rely on single or multivariate polynomial regressors, such as Lyzenga's model [38], [39] or band ratio techniques [17], [40]. These regression models require selection of spectral features, such as log-transformed single bands or band ratios; the choice of bands can affect the depth estimates. Machine learning approaches have rarely been utilized for fluvial bathymetry retrieval [6]. Here, we employ NNs for depth retrieval to account for nonlinear relationships between multiband spectral data and *in situ* depth measurements. NN-based models can capture informative features without prior feature extraction [31], [41]. Our NN architecture builds upon two feedforward fully connected layers. The first fully connected layer is connected to the network input data, which are the spectra from training samples. Each fully connected layer multiplies the input by a weight matrix, followed by the addition of a bias vector. An activation layer follows the first fully connected layer. The last fully connected layer produces the output, which is the water depth (see Fig. 1). The hyperparameters of the network, including the number of layers, size of each layer (number of neurons), and the type of activation functions, including rectified linear unit, sigmoid, and hyperbolic tangent, are tuned in an iterative procedure to minimize the cross-validation error. This tuning experiment indicated that networks with two hidden layers provided robust retrievals. Given that imagery from sensors with various spectral, radiometric, and spatial resolutions was analyzed in this study, the other hyperparameters of the network were optimized individually for each type of image. The training is repeated ten times, and the average of the estimated depths is provided as the final retrieval.

To assess the extent to which Landsat-9's high-resolution panchromatic band with 15 m pixels might enhance bathymetry retrieval, we examine the effect of pan-sharpening by comparing the results obtained using pan-sharpened images with those derived from the original (30 m) data. Pan-sharpening is a fusion approach that integrates the geometric information from the panchromatic band with the spectral information from the multispectral bands to provide a high-resolution multispectral image [42]. We employ a widely used pan-sharpening method called Gram-Schmidt [43] to enhance the spatial resolution of Landsat-9 imagery, which could greatly extend the utility of these data in fluvial systems, given the narrow channel width of most rivers. This pan-sharpening method demonstrated promising results in a previous study on satellite-based mapping of river bathymetry [16]. The Sentinel-2 bands are acquired with different spatial resolutions (10–60 m). A standard approach available in the Sentinel Application Platform software is used to resample all the bands to the highest possible spatial resolution of 10 m. The upsampling to finer spatial resolution is performed by bilinear interpolation. We investigate the bathymetry retrieval with the original spatial resolution of imagery from different

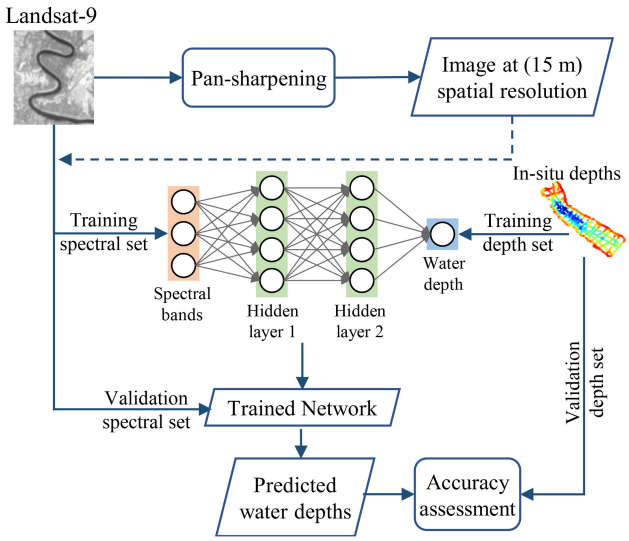

Fig. 5. Schematic representation of the workflow for depth retrieval based on the NN model at either original or pan-sharpened (dashed line) resolutions of Landsat-9 imagery. The layer sizes are only for visualization.

sensors, i.e., 30-m Landsat-9, 10-m Sentinel-2, and 3-m SuperDove. However, to isolate the impact of spatial resolution, we resample the imagery from SuperDoves and Sentinel-2 to a common spatial resolution of 15 m comparable to the pan-sharpened Landsat-9 imagery. The pixel values are averaged for downsampling the imagery to the coarser (15-m) resolution. For cases where the downsampling scale factor is not an integer (e.g., 10 m Sentinel-2 pixels downsampled to 15 m), the proportion of the original pixels within the coarser downsampled pixels is used as an averaging weight to perform the pixel aggregation. Downsampling the images brings another interesting aspect to our research, as this procedure can enhance the SNR by averaging pixels [2]. The impact of downsampling on depth retrieval, relative to the original coarser-resolution image, is expected to be more pronounced for SuperDove with a very high spatial resolution. Fig. 5 shows a schematic representation of the proposed workflow to retrieve the bathymetry based on training NN at original and pan-sharpened resolutions of Landsat-9 imagery. The validation is performed based on independent *in situ* data. The same workflow is applied to imagery from the other sensors at both their original and resampled resolutions, excluding the pan-sharpening step.

We compare the NN model with the standard OBRA method that has been well-documented in the literature [17]. OBRA examines all possible log-transformed band ratios (X) to find the one providing the highest R^2 in a regression of X against the water depth (d). Different forms of regression models (e.g., linear, quadratic, exponential, and power-law) can be applied, depending on the range of depths and the degree of curvature in the X versus d relation. In this study, an exponential model is considered for OBRA, as it performed better than the other forms in previous studies [6].

In all experiments with either NN or OBRA, half of the *in situ* samples were selected at random and used for training the models; the remaining half was reserved for validation [44]. *In situ* matchup scatterplots (i.e., regressing *in situ* depths versus predicted depths) provided a set of metrics to quantify the accuracy of retrievals. We evaluated the R^2, root mean square error (RMSE), mean absolute error (MAE), and bias of depth estimates. A log-transformed space is considered for the calculation of MAE and bias to account for the proportionality of errors with the water depth [45]. Bias values close to 1 imply minimal systematic errors. Bias >1 and bias <1 indicate overestimation and underestimation of bathymetry, respectively. For instance, a bias of 1.1 implies that estimated depths are on average 10% overestimated with respect to the reference field data. MAE indicates the relative error of depth estimation and always exceeds one. Bias and MAE are both unitless. The accuracy metrics are formulated in (1)−(4), where n stands for the total number of estimated values and E_i and O_i are the estimated and field-measured values, respectively

$$R^2 = \frac{\sum_{i=1}^{n}\left(E_i-\bar{O}\right)^2}{\sum_{i=1}^{n}\left(O_i-\bar{O}\right)^2}\,,\quad \bar{O}=\frac{1}{n}\sum_{i=1}^{n}O_i \tag{1}$$

$$\text{RMSE} = \left(\frac{\sum_{i=1}^{n}\left(E_i-O_i\right)^2}{n}\right)^{1/2} \tag{2}$$

$$\text{bias} = 10^{\frac{\sum_{i=1}^{n}\log_{10}(E_i/O_i)}{n}} \tag{3}$$

$$\text{MAE} = 10^{\frac{\sum_{i=1}^{n}\left|\log_{10}(E_i/O_i)\right|}{n}}. \tag{4}$$

IV. Results and Discussion

In this section, we provide the results of depth retrieval from Landsat-9, 8-band SuperDove, 4-band SuperDove, and Sentinel-2 at original and pan-sharpened/resampled spatial resolutions. Matchup scatterplots and accuracy statistics are provided for the validation samples. Moreover, bathymetric maps are produced for the study reaches. For brevity, the results of OBRA are presented in less detail, as OBRA provided less accurate results than the NN model. However, all accuracy statistics are reported.

A. Colorado River

An example of OBRA from the Landsat-9 image of the Colorado River is provided in Fig. 6. The colors on the OBRA matrix [see Fig. 6(a)] represent the training R^2 for all possible band combinations to build the ratio model. The blue (443 nm) to green (561 nm) ratio model provided the optimal results (validation $R^2 = 0.48$ and RMSE $= 2.44$ m).

The validation based on independent *in situ* matchups [see Fig. 6(b)] indicates that the bathymetry retrieval fails for depths >10 m. The water depth in the Colorado site spans a wide range (up to $\sim$20 m) that prevents a single band ratio model from achieving reliable results across the entire range of depths. This highlights the importance of incorporating all of the available spectral information in depth retrieval through methods like NNs.

The scatterplots of *in situ* versus retrieved depths based on the NN model are shown in Fig. 7 for various types of imagery at original and pan-sharpened/resampled resolutions. Landsat-9

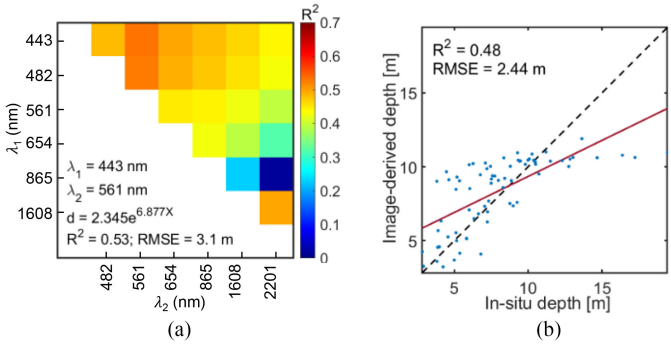

Fig. 6. (a) OBRA of Landsat-9 image over Colorado River representing training R^2 for all possible combinations of the numerator (λ_1) and denominator (λ_2) bands along with (b) *in situ* matchup validation.

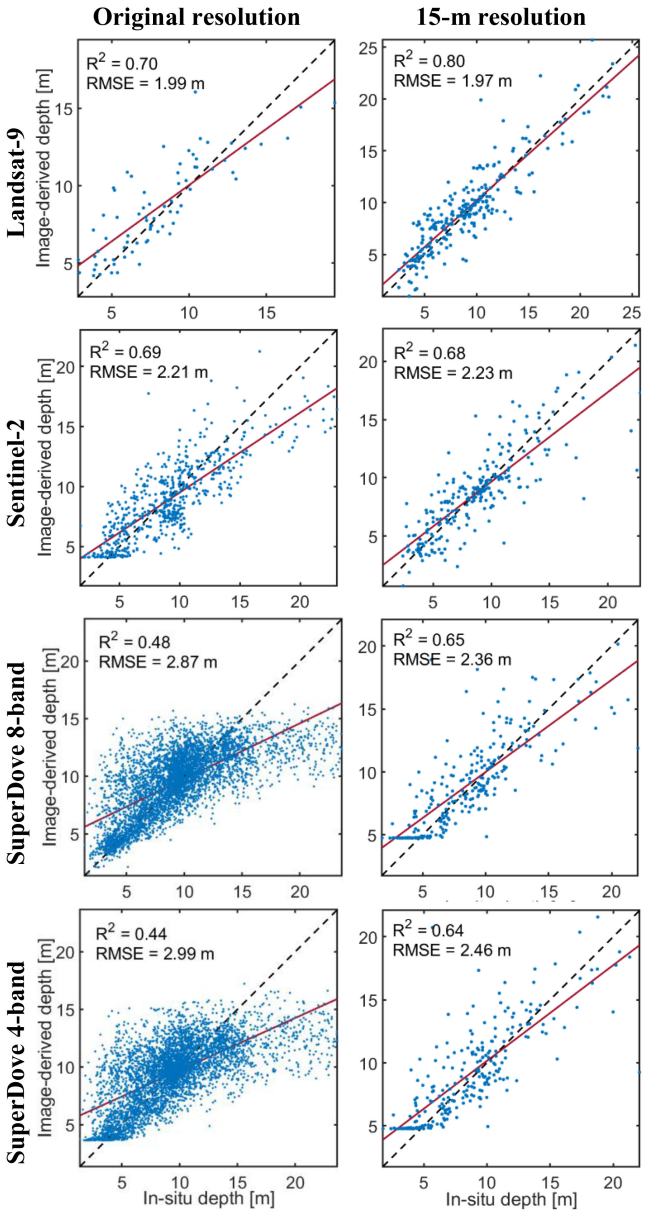

Fig. 7. *In situ* matchup validation of bathymetry retrieval from different satellite images from the Colorado River based on the NN method.

TABLE II
ACCURACY STATISTICS DERIVED FROM *IN SITU* MATCHUP VALIDATION OF BATHYMETRY RETRIEVAL FROM DIFFERENT SATELLITE IMAGES FROM THE COLORADO RIVER BASED ON NN AND OBRA MODELS

	R^2		RMSE [m]		MAE [m]		Bias	
	NN	**OBRA**	**NN**	**OBRA**	**NN**	**OBRA**	**NN**	**OBRA**
Landsat-9 (30 m)	0.70	0.48	1.99	2.44	1.19	1.21	1.01	0.96
Landsat-9 (15 m)	0.80	0.36	1.97	3.16	1.20	1.31	1.03	1.02
Sentinel 2 (10 m)	0.69	0.38	2.21	3.5	1.18	1.33	0.99	0.96
Sentinel-2 (15 m)	0.68	0.37	2.23	3.13	1.22	1.29	0.99	0.99
SuperDove 8-band (3 m)	0.48	0.27	2.87	3.44	1.24	1.32	1.04	1.02
SuperDove 8-band (15 m)	0.65	0.46	2.36	2.89	1.22	1.26	1.05	1.04
SuperDove 4-band (3 m)	0.44	0.27	2.99	3.44	1.26	1.32	1.04	1.03
SuperDove 4-band (15 m)	0.64	0.46	2.46	2.89	1.21	1.25	1.05	1.03

yields the highest accuracies either at the original (30 m) or the pan-sharpened (15 m) resolution, with the pan-sharpened image providing the highest accuracy ($R^2 = 0.8$ and RMSE $= 1.97$ m). The results from Sentinel-2 are slightly less accurate than those of Landsat-9 (RMSE $= 2.21$ m). An interesting point about the SuperDove-based results is that estimates for depths > 15 m are not accurate at the original spatial resolution (3 m), whereas downsampling the images to 15 m substantially improves the depth retrieval and captures the deep waters. The depth retrieval based on 8-band SuperDove data at 15-m resolution provided an R^2 of 0.65 and RMSE of 2.36 m, comparable to those of Sentinel-2 ($R^2 = 0.68$ and RMSE $= 2.23$). The improved retrieval of bathymetry at the downsampled resolution, particularly from deeper water with lower reflectance, can be attributed to an enhanced SNR resulting from the pixel-averaging process [2], [46], [47]. The averaging reduces noise, which can be sizable in high-spatial resolution imagery [48]. Given that the water-leaving signal over deep waters is so low, any small noise can be a significant portion of the signal. Thus, reducing noise by averaging the pixels leads to a pronounced improvement of the SNR, which is critical for retrieving bathymetry in deeper areas. Another key point is that the additional bands of 8-band SuperDove improved depth retrieval compared to 4-band classic Doves (0.12 m and 0.1 m improvement of RMSE for the original and resampled data, respectively). Fig. 7 implies that shallow areas were not well characterized. We attribute this issue to a lack of training samples from shallow areas. The accuracy statistics derived from the validation analyzes are reported in Table II; OBRA-based retrievals are poor compared to the NN model. The average biases are close to 1 and thus could be considered negligible for all cases. The NN-based statistics confirm the high accuracy of retrievals from Landsat-9, but the other sensors also provide accurate estimates.

Fig. 8 compares the NN-based bathymetry maps derived from different sensors at both the original and pan-sharpened/resampled resolutions. The Landsat-9 map at original resolution is relatively coarse, whereas the map derived from the pan-sharpened image shows detailed bathymetric information. Visual inspection indicates that the maps from different sensors

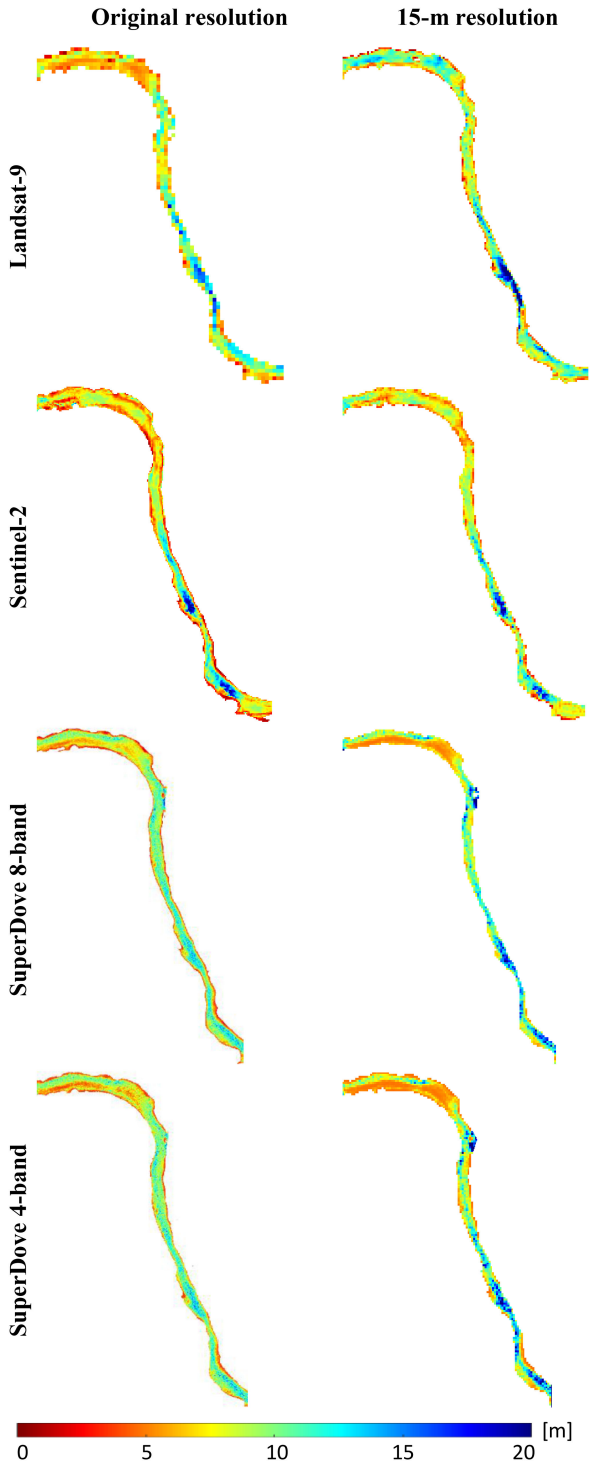

Fig. 8. Bathymetry maps derived from different satellite imagery in Colorado River based on the NN model.

agree well. However, the maps derived from SuperDove imagery at the original resolution fail to accurately capture the deepest areas of the channel. As mentioned above, these errors can be attributed to the low SNR in deep pools.

In these clear-flowing rivers, the water-leaving radiance signal of interest decreases as water depth increases due to strong absorption of solar radiation by the water column. However, the deep waters (up to 20 m) are mapped plausibly by downsampling the SuperDove data to 15-m resolution due to enhanced SNR, which is in line with matchup analysis (see Fig. 7).

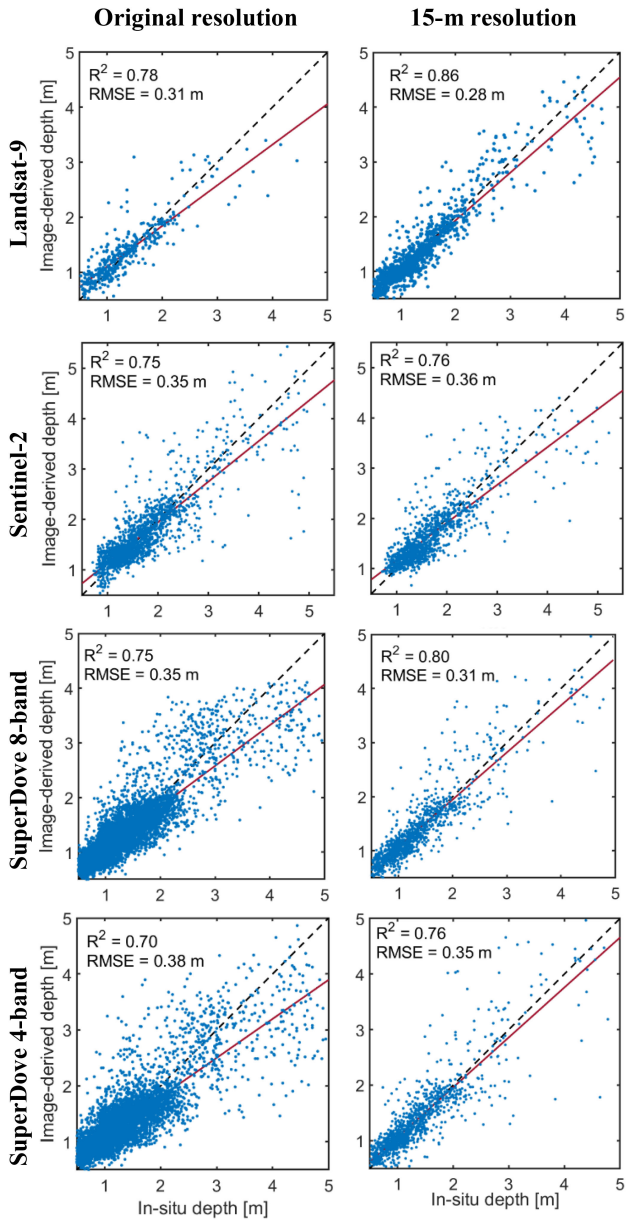

Fig. 9. *In situ* matchup validation of bathymetry retrieval from different satellite images from the Potomac River based on the NN method.

B. Potomac River

The results from the Potomac River also demonstrate improved depth retrieval when using Landsat-9 imagery compared to the other sensors (see Fig. 9). Similar to the Colorado site, depth retrieval benefited from pan-sharpening (R^2 of 0.86 versus 0.78 for the original image). Sentinel-2 and SuperDove also provided comparable results to those of Landsat-9. The downsampled SuperDove data led to improvements in this river, as in the Colorado. Moreover, the 8-band CubeSat data provided improvements compared to the 4-band data (see Fig. 9).

TABLE III
ACCURACY STATISTICS DERIVED FROM *IN SITU* MATCHUP VALIDATION OF BATHYMETRY RETRIEVAL FROM DIFFERENT SATELLITE IMAGERY IN POTOMAC RIVER BASED ON NN AND OBRA MODELS

	R^2		RMSE [m]		MAE [m]		Bias	
	NN	OBRA	NN	OBRA	NN	OBRA	NN	OBRA
Landsat-9 (30 m)	0.78	0.12	0.31	0.64	1.16	1.39	1.03	1.02
Landsat-9 (15 m)	0.86	0.35	0.28	0.66	1.14	1.37	1.01	1.01
Sentinel 2 (10 m)	0.75	0.10	0.35	0.72	1.15	1.33	1.01	1.01
Sentinel-2 (15 m)	0.76	0.09	0.36	0.71	1.15	1.32	1.01	0.98
SuperDove 8-band (3 m)	0.75	0.24	0.35	0.61	1.18	1.34	1.01	0.99
SuperDove 8-band (15 m)	0.80	0.15	0.31	0.65	1.16	1.41	1.03	1.04
SuperDove 4-band (3 m)	0.70	0.06	0.38	0.69	1.20	1.37	1.02	0.99
SuperDove 4-band (15 m)	0.76	0.14	0.35	0.65	1.17	1.41	1.02	1.04

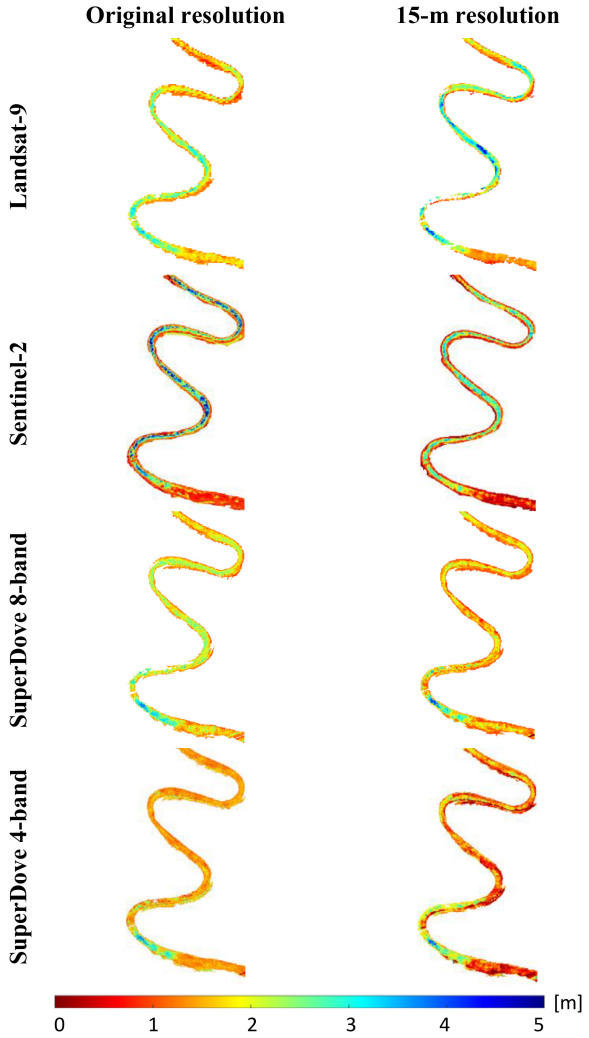

Fig. 10. Bathymetry maps derived from different satellite images from the Potomac River based on NN.

The *in situ* matchup analysis is quantified in Table III, which indicate that the NN model outperforms OBRA in all cases. The best result is achieved by applying the NN model on the pan-sharpened Landsat-9 image ($R^2 = 0.86$ and RMSE = 0.28 m).

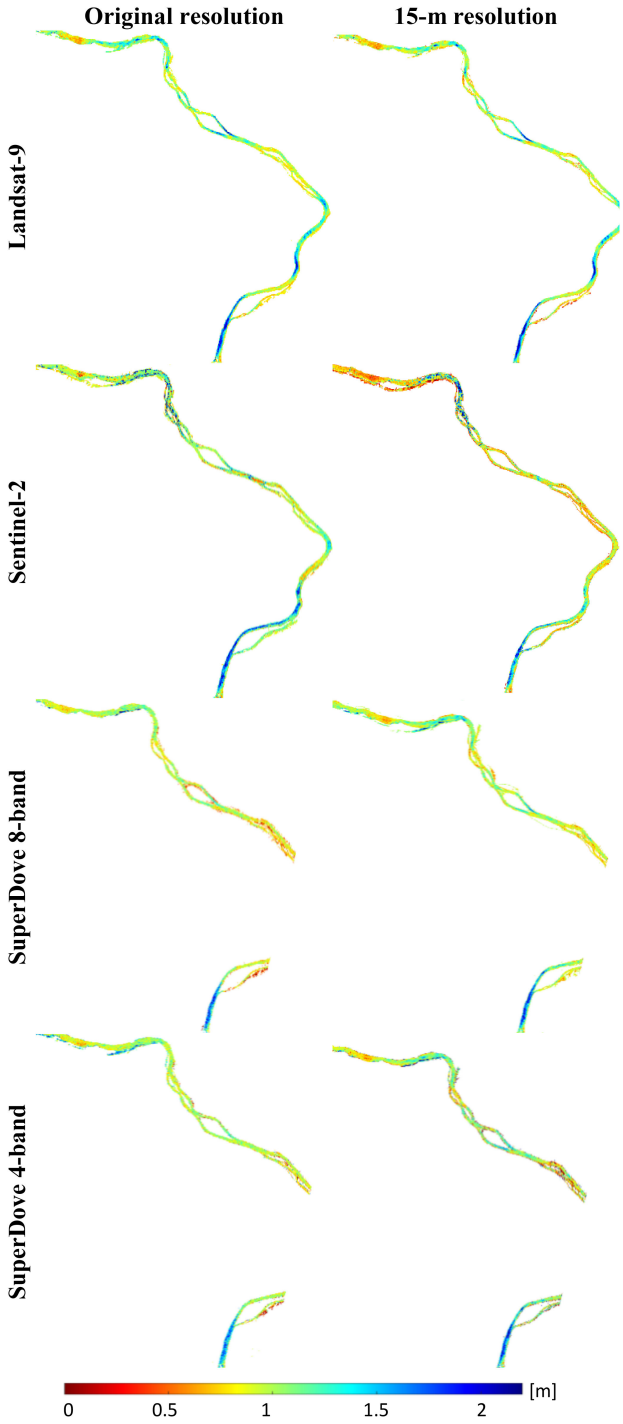

Fig. 11. Bathymetry maps derived from different satellite images from the Potomac River based on NN.

The NN-based bathymetry maps are shown for two subsets of the imagery in Figs. 10 and 11. As the Sentinel-2 image was acquired at a different flow stage, we removed the gage level shift with respect to the other images to enable visual comparison of the maps.

The maps show relatively good agreement across the full range of depths, which is also confirmed by the matchup analyzes (see Fig. 9).

Despite the time gap between image and field data acquisition, the high accuracies ($R^2 > 0.8$) achieved for depth retrieval in both case studies imply that the *in situ* data are highly reliable. If a major change in the bed topography had occurred, the depth estimates would have been much less accurate. This result further confirms that regulation of the rivers by dams essentially precluded any major changes in the channel. In addition, any possible small impact due to channel change would have affected the depth retrieval from different sensors similarly and thus does not influence our overall results.

V. Conclusion and Areas for Additional Research

A boom in the availability of different satellite image data sources is currently underway, creating a compelling incentive to investigate their potential to facilitate aquatic applications. Landsat-9 (OLI-2) with a 14-bit dynamic range and, on the other hand, SuperDoves with meter-scale resolution and daily acquisitions open up a new era for monitoring inland waters. This study provided the first assessment of the potential of these new image data sources for retrieving river bathymetry across a broad range of water depths (up to $\sim$20 m). We leveraged a machine learning-based model for depth retrieval based on NNs and compared the results with those from standard OBRA. In addition, the impact on bathymetric mapping of Landsat-9 pan-sharpening and downsampling of high spatial resolution imagery were investigated.

The NN-based model outperformed standard OBRA in all experiments. OBRA relies on a single band ratio, whereas the NN model takes advantage of all spectral bands. Moreover, NNs do not require *a priori* selection of features and can identify informative and robust features from the original bands. These characteristics of NN explain the superior performance relative to OBRA. Landsat-9, particularly pan-sharpened images, provided the most accurate bathymetry retrieval. Downsampling SuperDove pixels by a factor of five (from 3 to 15 m) significantly improved depth estimation, particularly in deep parts (> 15 m) of the Colorado River. The noticeable improvements in depth retrieval in deeper areas suggest that the pixel averaging involved in spatial downsampling might enhance the SNR. Because deeper water tends to be less reflective in clear-flowing streams, an enhanced SNR can improve the sensitivity of imagery data to subtle changes in water-leaving radiance and thus extend the range of depths detectable. The resampled (15 m) SuperDove data provided results comparable to Sentinel-2 and Landsat-9. The enhanced spectral resolution of the 8-band SuperDoves compared to classic 4-band doves also improved the results.

Although we examined depth retrieval from new Landsat-9 and SuperDove data using field measurements spanning a broad range of depths, aquatic scientists, and water managers would benefit from further investigations in additional streams elsewhere, as well as in water bodies other than rivers, such as lakes and coastal waters. In this study, we employed an NN-based method. However, other machine learning methods (e.g., support vector machines) could also be considered. Moreover, future studies could address physics-based approaches that require accurate atmospheric correction of the imagery. This kind of physics-based modeling can give further insight regarding the data quality of different sensors. Although we relied on the widely-used Gram–Schmidt method, future studies can investigate the impact of different techniques for pan-sharpening Landsat-9 imagery. Assessment of these new sources of imagery in other aquatic applications (e.g., water quality retrieval and benthic habitat mapping) would also be interesting topics to explore.

Acknowledgment

The authors would like to thank Planet Inc.'s Education and Research Program that provided us with the SuperDove imagery. Any use of trade, firm, or product names is for descriptive purposes only and does not imply endorsement by the U.S. Government.

References

[1] J. G. Masek *et al.*, "Landsat 9: Empowering open science and applications through continuity," *Remote Sens. Environ.*, vol. 248, Oct. 2020, Art. no. 111968.

[2] A. D. Gerace, J. R. Schott, and R. Nevins, "Increased potential to monitor water quality in the near-shore environment with Landsat's next-generation satellite," *J. Appl. Remote Sens.*, vol. 7, no. 1, pp. 1–19, 2013.

[3] V. Markogianni, D. Kalivas, G. Petropoulos, and E. Dimitriou, "An appraisal of the potential of Landsat 8 in estimating Chlorophyll-a, ammonium concentrations and other water quality indicators," *Remote Sens.,* vol. 10, no. 7, Jun. 2018, Art. no. 1018.

[4] C. Giardino *et al.*, "Imaging spectrometry of inland and coastal waters: State of the art, achievements and perspectives," *Surv. Geophys.*, vol. 40, no. 3, pp. 401–429, 2019.

[5] J. R. Schott *et al.*, "The impact of improved signal-to-noise ratios on algorithm performance: Case studies for Landsat class instruments," *Remote Sens. Environ.*, vol. 185, pp. 37–45, 2016.

[6] C. J. Legleiter and L. R. Harrison, "Remote sensing of river bathymetry: Evaluating a range of sensors, platforms, and Algorithms on the Upper Sacramento River, California, USA," *Water Resour. Res.*, vol. 55, no. 3, pp. 2142–2169, Mar. 2019.

[7] W. A. Marcus and M. Fonstad, "Remote sensing of rivers: The emergence of a subdiscipline in the river sciences," *Earth Surf. Process. Landforms*, vol. 35, no. 15, pp. 1867–1872, 2010.

[8] M. Niroumand-Jadidi and F. Bovolo, "Water quality retrieval and Algal bloom detection using high-resolution Cubesat imagery," *ISPRS Annu. Photogrammetry Remote Sens. Spatial Inf. Sci.*, vol. 3, pp. 191–195, Jun. 2021.

[9] M. Niroumand-Jadidi, F. Bovolo, L. Bruzzone, and P. Gege, "Physics-based bathymetry and water quality retrieval using planetscope imagery: Impacts of 2020 COVID-19 lockdown and 2019 extreme flood in the venice lagoon," *Remote Sens.,* vol. 12, no. 15, Jul. 2020, Art. no. 2381.

[10] D. P. Roy, H. Huang, R. Houborg, and V. S. Martins, "A global analysis of the temporal availability of planetscope high spatial resolution multi-spectral imagery," *Remote Sens. Environ.*, vol. 264, Oct. 2021, Art. no. 112586.

[11] D. Poursanidis, D. Traganos, N. Chrysoulakis, and P. Reinartz, "Cubesats allow high spatiotemporal estimates of satellite-derived bathymetry," *Remote Sens.,* vol. 11, no. 11, May 2019, Art. no. 1299.

[12] K. Toming, T. Kutser, A. Laas, M. Sepp, B. Paavel, and T. Nõges, "First experiences in mapping lake water quality parameters with sentinel-2 MSI imagery," *Remote Sens.,* vol. 8, no. 8, Aug. 2016, Art. no. 640.

[13] M. Niroumand-Jadidi, A. Vitti, and D. R. Lyzenga, "Multiple optimal depth predictors analysis (MODPA) for river bathymetry: Findings from spectroradiometry, simulations, and satellite imagery," *Remote Sens. Environ.*, vol. 218, pp. 132–147, Dec. 2018.

[14] J. Gao, "Bathymetric mapping by means of remote sensing: Methods, accuracy and limitations," *Prog. Phys. Geography Earth Environ.*, vol. 33, no. 1, pp. 103–116, Feb. 2009.

[15] M. Niroumand-Jadidi, F. Bovolo, and L. Bruzzone, "SMART-SDB: Sample-specific multiple band ratio technique for satellite-derived bathymetry," *Remote Sens. Environ.*, vol. 251, Dec. 2020, Art. no. 112091.
[16] C. J. Legleiter and B. T. Overstreet, "Mapping gravel bed river bathymetry from space," *J. Geophys. Res. Earth Surf.*, vol. 117, no. 4, pp. 1–24, 2012.
[17] C. J. Legleiter, D. A. Roberts, and R. L. Lawrence, "Spectrally based remote sensing of river bathymetry," *Earth Surf. Process. Landforms*, vol. 34, no. 8, pp. 1039–1059, Jun. 2009.
[18] F. Visser, K. Buis, V. Verschoren, and P. Meire, "Depth estimation of submerged aquatic vegetation in clear water streams using low-altitude optical remote sensing," *Sensors*, vol. 15, no. 10, pp. 25287–25312, Sep. 2015.
[19] I. Caballero and R. P. Stumpf, "Retrieval of nearshore bathymetry from Sentinel-2A and 2B satellites in South Florida coastal waters," *Estuarine Coastal Shelf Sci.*, vol. 226, Oct. 2019, Art. no. 106277.
[20] I. Caballero and R. P. Stumpf, "Towards routine mapping of shallow bathymetry in environments with variable turbidity: Contribution of Sentinel-2A/B satellites mission," *Remote Sens.*, vol. 12, no. 3, Feb. 2020, Art. no. 451.
[21] G. Casal, X. Monteys, J. Hedley, P. Harris, C. Cahalane, and T. McCarthy, "Assessment of empirical algorithms for bathymetry extraction using Sentinel-2 data," *Int. J. Remote Sens.*, vol. 40, no. 8, pp. 2855–2879, Apr. 2019.
[22] C. E. Simpson, C. D. Arp, Y. Sheng, M. L. Carroll, B. M. Jones, and L. C. Smith, "Landsat-derived bathymetry of lakes on the arctic coastal plain of northern Alaska," *Earth Syst. Sci. Data*, vol. 13, no. 3, pp. 1135–1150, Mar. 2021.
[23] B. Gabr, M. Ahmed, and Y. Marmoush, "PlanetScope and Landsat 8 imageries for bathymetry mapping," *J. Mar. Sci. Eng.*, vol. 8, no. 2, Feb. 2020, Art. no. 143.
[24] P. Gege, "The water color simulator WASI: An integrating software tool for analysis and simulation of optical *in situ* spectra," *Comput. Geosci.*, vol. 30, no. 5, pp. 523–532, Jun. 2004.
[25] C. D. Mobley, *Light and Water : Radiative Transfer in Natural Waters*. Cambridge, MA, USA: Academic, 1994.
[26] P. Gege, "Chapter 2 - Radiative transfer theory for inland waters," in *Bio-Optical Modeling and Remote Sensing of Inland Waters*, D. R. Mishra, I. Ogashawara, and A. A. Gitelson, Eds. Amsterdam, The Netherlands: Elsevier, 2017, pp. 25–67.
[27] M. Niroumand-Jadidi, F. Bovolo, L. Bruzzone, and P. Gege, "Inter-comparison of methods for chlorophyll—A retrieval: Sentinel-2 time-series analysis in Italian lakes," *Remote Sens.,* vol. 13, no. 12, Jun. 2021, Art. no. 2381.
[28] P. Gege, "WASI-2D: A software tool for regionally optimized analysis of imaging spectrometer data from deep and shallow waters," *Comput. Geosci.*, vol. 62, pp. 208–215, Jan. 2014.
[29] C. Giardino, G. Candiani, M. Bresciani, Z. Lee, S. Gagliano, and M. Pepe, "BOMBER: A tool for estimating water quality and bottom properties from remote sensing images," *Comput. Geosci.*, vol. 45, pp. 313–318, Aug. 2012.
[30] E. Kasvi, J. Salmela, E. Lotsari, T. Kumpula, and S. N. Lane, "Comparison of remote sensing based approaches for mapping bathymetry of shallow, clear water rivers," *Geomorphology*, vol. 333, pp. 180–197, May 2019.
[31] F. Murtagh, "Multilayer perceptrons for classification and regression," *Neurocomputing*, vol. 2, no. 5/6, pp. 183–197, Jul. 1991.
[32] P. J. Kinzel, C. J. Legleiter, and P. E. Grams, Remotely Sensed Bathymetry and Field Measurements From the Colorado River Near Lees Ferry, Arizona, September 23, 2019: U.S. Geological Survey Data Release. U.S. Geological Survey, Golden, CO, USA, 2021.
[33] J. M. Duda, A. J. Greise, and J. A. Young, *Potomac river ADCP bathymetric survey, October 2019*, *U.S. Geological Survey Data Release*, Golden, CO, USA, 2020.
[34] T. Harmel, M. Chami, T. Tormos, N. Reynaud, and P. A. Danis, "Sunglint correction of the multi-spectral instrument (MSI)-SENTINEL-2 imagery over inland and sea waters from SWIR bands," *Remote Sens. Environ.*, vol. 204, pp. 308–321, Jan. 2018.
[35] Q. Vanhellemont, "Adaptation of the dark spectrum fitting atmospheric correction for aquatic applications of the Landsat and Sentinel-2 archives," *Remote Sens. Environ.*, vol. 225, pp. 175–192, May 2019.
[36] J. Martin, F. Eugenio, J. Marcello, and A. Medina, "Automatic sun glint removal of multispectral high-resolution worldview-2 imagery for retrieving coastal shallow water parameters," *Remote Sens.,* vol. 8, no. 1, 2016, Art. no. 37.
[37] Q. Vanhellemont, "acolite/data/RSR at main acolite/acolite github," 2022, Accessed: May 9, 2022. [Online]. Available: https://github.com/acolite/acolite/tree/main/data/RSR
[38] D. R. Lyzenga, "Passive remote sensing techniques for mapping water depth and bottom features," *Appl. Opt.*, vol. 17, no. 3, Feb. 1978, Art. no. 379.
[39] D. R. Lyzenga, N. P. Malinas, and F. J. Tanis, "Multispectral bathymetry using a simple physically based Algorithm," *IEEE Trans. Geosci. Remote Sens.*, vol. 44, no. 8, pp. 2251–2259, Aug. 2006.
[40] R. P. Stumpf, K. Holderied, and M. Sinclair, "Determination of water depth with high-resolution satellite imagery over variable bottom types," *Limnology Oceanogr.*, vol. 48, no. 1, pp. 547–556, Jan. 2003.
[41] F. Shaheen, B. Verma, and M. Asafuddoula, "Impact of automatic feature extraction in deep learning architecture," in *Proc. Int. Conf. Digit. Image Comput. Tech. Appl.*, Dec. 2016, pp. 638–645.
[42] X. Meng, H. Shen, H. Li, L. Zhang, and R. Fu, "Review of the pansharpening methods for remote sensing images based on the idea of meta-analysis: Practical discussion and challenges," *Inf. Fusion*, vol. 46, pp. 102–113, Mar. 2019.
[43] C. A. Laben and B. V. Brower, "Process for enhancing the spatial resolution of multispectral imagery using pan-sharpening," U.S. Patent 6,011,875, 2000.
[44] E. Pontoglio, N. Grasso, A. Cagninei, C. Camporeale, P. Dabove, and M. Lingua Andrea, "Bathymetric detection of fluvial environments through UASs and machine learning systems," *Remote Sens.*, vol. 12, no. 24, Dec. 2020, Art. no. 4148.
[45] B. N. Seegers, R. P. Stumpf, B. A. Schaeffer, K. A. Loftin, and P. J. Werdell, "Performance metrics for the assessment of satellite data products: An ocean color case study," *Opt. Exp.*, vol. 26, no. 6, pp. 7404–7422, Mar. 2018.
[46] Q. Vanhellemont and K. Ruddick, "Advantages of high quality SWIR bands for ocean colour processing: Examples from Landsat-8," *Remote Sens. Environ.*, vol. 161, pp. 89–106, May 2015.
[47] D. S. F. Jorge *et al.*, "SNR (signal-to-noise ratio) impact on water constituent retrieval from simulated images of optically complex Amazon lakes," *Remote Sens.*, vol. 9, no. 7, Jun. 2017, Art. no. 644.
[48] F. L. Hellweger, P. Schlosser, U. Lall, and J. K. Weissel, "Use of satellite imagery for water quality studies in New York Harbor," *Estuarine Coastal Shelf Sci.*, vol. 61, no. 3, pp. 437–448, 2004.

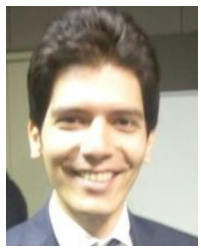

Milad Niroumand-Jadidi (Member, IEEE) received the B.Sc. degree in geomatics engineering from the University of Tabriz, Tabriz, Iran, in 2009, the M.Sc. degree in remote sensing engineering from the K.N. Toosi University of Technology, Tehran, Iran, in 2013, and the Ph.D. degree in civil and environmental engineering from the University of Trento, Italy, and Freie Universität Berlin, Berlin, Germany, in 2017.

Since 2017, he has been a Postdoctoral Researcher with the Remote Sensing for Digital Earth (RSDE), Digital Society Center, Fondazione Bruno Kessler (FBK), Trento, Italy. He has authored or coauthored more than ten peer-reviewed articles in top journals and presented numerous papers at international conferences. His main research interests include the development of methods and applications for remote sensing of inland and coastal waters from optical data. He focuses on both physics-based and machine learning models to retrieve information on water quality and bathymetry.

Dr. Niroumand-Jadidi was the recipient of several international awards and a DLR-DAAD fellowship for spending three months (May−August 2022) as a Visiting Scientist with the German Aerospace Center (DLR). He was also the recipient of the Best Young Author Award from the International Society for Photogrammetry and Remote Sensing (ISPRS) in 2021 and the best paper award from SPIE Remote Sensing conferences for three years in a row (2015 in Toulouse, 2016 in Edinburgh, and 2017 in Warsaw). He is a recipient of the award for potential long-range contribution to the field of optics and photonics from the International Society for Optics and Photonics (SPIE) in 2016 and Alexander Goetz Instrument Support Award 2016, which gave him access to a field spectroradiometer during his Ph.D. research. He serves on the editorial board for the journal *Remote Sensing* and has also been a special issue editor. He is a referee for several international journals, including IEEE TRANSACTIONS ON GEOSCIENCE AND REMOTE SENSING, *Remote Sensing of Environment*, *Remote Sensing*, *Journal of Hydrology, Water*, and *International Journal of Remote Sensing*.

Carl J. Legleiter received the B.S. degrees in earth sciences and mathematical sciences from Montana State University, Bozeman, MT, USA, in 2002 and the M.A. and Ph.D. degrees in geography from the University of California, Santa Barbara, Santa Barbara, CA, USA, in 2004 and 2008, respectively.

He was a Research Hydrologist with the U.S. Geological Survey in 2009 and became an Assistant Professor of Geography with the University of Wyoming, Laramie, WY, USA, later that year. He was promoted to Associate Professor in 2015 and returned to the U.S. Geological Survey in 2016. Since that time, he has been a Research Hydrologist with the Geomorphology and Sediment Transport Laboratory, Golden, CO, USA. He has authored or coauthored nearly 100 peer-reviewed articles in top journals, as well as numerous data releases. In addition, he has presented or been a coauthor of more than 60 papers at international conferences. His main research interests include developing methods for characterizing various aspects of rivers via remote sensing. He is currently focused on spectrally based bathymetric mapping, inference of flow velocity from image time series, retrieving tracer dye concentrations to enhance dispersion studies, and detecting algal blooms.

Dr. Legleiter was the recipient of several awards, including a National Defense Science and Engineering from the American Society for Engineering Education, a Graduate Research Fellowship from the National Science Foundation, and a Canon National Parks Science Scholars Fellowship. After joining the University of Wyoming, he earned major research and instrumentation grants from the Office of Naval Research as well as numerous smaller grants. Most recently, he is currently the Principal Investigator on a new project focused on the use of uncrewed aircraft systems for real-time measurement of surface flow velocities funded by the National Aeronautics and Space Administration's Advanced Information Systems Technology program. He currently serves on the editorial board for *Geomorphology* and has also been a member of the editorial board for *Remote Sensing*. In addition, he organized a conference on "The Field Tradition in Geomorphology" and a special issue of Remote Sensing on remote sensing of river discharge. He is a referee for several international journals, including Water Resources Research, Geomorphology, Earth Surface Processes and Landforms, IEEE TRANSACTIONS ON GEOSCIENCE AND REMOTE SENSING, *Remote Sensing of Environment*, and *Remote Sensing*.

Francesca Bovolo (Senior Member, IEEE) received the Laurea (B.S.) degree, the Laurea Specialistica (M.S.) degree (*summa cum laude*) in telecommunication engineering, and the Ph.D. degree in communication and information technologies from the University of Trento, Trento, Italy, in 2001, 2003, and 2006, respectively.

She was a Research Fellow with the University of Trento, until 2013. She is currently the Founder and the Head of Remote Sensing for Digital Earth Unit, Fondazione Bruno Kessler, Trento, Italy, and a member of the Remote Sensing Laboratory, Trento, Italy. She is one of the Co-Investigators of the Radar for Icy Moon Exploration instrument of the European Space Agency Jupiter Icy Moons Explorer and member of the science study team of the EnVision mission to Venus. She conducts research on these topics within the context of several national and international projects. Her research interests include remote-sensing image processing, multitemporal remote sensing image analysis, change detection in multispectral, hyperspectral, and synthetic aperture radar images and very high-resolution images, time series analysis, content-based time series retrieval, domain adaptation, and light detection and ranging and radar sounders.

Dr. Bovolo is a Member of the program and scientific committee of several international conferences and workshops. She was the recipient of the First Place in the Student Prize Paper Competition of the 2006 IEEE International Geoscience and Remote Sensing Symposium (Denver, 2006). She was the Technical Chair of the Sixth InternationalWorkshop on the Analysis of Multitemporal Remote-Sensing Images (MultiTemp 2011, and 2019). She has been a Co-Chair of the SPIE International Conference on Signal and Image Processing for Remote Sensing since 2014. She is the Publication Chair for the International Geoscience and Remote Sensing Symposium in 2015. She has been an Associate Editor for the IEEE JOURNAL OF SELECTED TOPICS IN APPLIED EARTH OBSERVATIONS AND REMOTE SENSING since 2011 and the Guest Editor of the Special Issue on Analysis of Multitemporal Remote Sensing Data of the IEEE TRANSACTIONS ON GEOSCIENCE AND REMOTE SENSING. She is a referee for several international journals.